JOURNAL OF AEROSOL MEDICINE AND PULMONARY DRUG DELIVERY
Volume 31, Number 3, 2018

Pp. 170–181
DOI: 10.1089/jamp.2017.1364

Hybrid Lipid/Polymer Nanoparticles for Pulmonary Delivery of siRNA: Development and Fate Upon *In Vitro* Deposition on the Human Epithelial Airway Barrier

Ivana d'Angelo, PhD,[1] Gabriella Costabile, PhD,[2,3] Estelle Durantie, PhD,[3] Paola Brocca, PhD,[4] Valeria Rondelli, PhD,[4] Annapina Russo, PhD,[5] Giulia Russo, PhD,[5] Agnese Miro, PharmD,[2] Fabiana Quaglia, PhD,[2] Alke Petri-Fink, PhD,[3] Barbara Rothen-Rutishauser, PhD,[3] and Francesca Ungaro, PhD[2]

Abstract

Background: Nowadays, the downregulation of genes involved in the pathogenesis of severe lung diseases through local siRNA delivery appears an interesting therapeutic approach. In this study, we propose novel hybrid lipid-polymer nanoparticles (hNPs) consisting of poly(lactic-co-glycolic) acid (PLGA) and dipalmitoyl phosphatidylcholine (DPPC) as siRNA inhalation system.

Methods: A panel of DPPC/PLGA hNPs was prepared by emulsion/solvent diffusion and fully characterized. A combination of model siRNAs against the sodium transepithelial channel (ENaC) was entrapped in optimized hNPs comprising or not poly(ethylenimine) (PEI) as third component. siRNA-loaded hNPs were characterized for encapsulation efficiency, release kinetics, aerodynamic properties, and stability in artificial mucus (AM). The fate and cytotoxicity of hNPs upon aerosolization on a triple cell co-culture model (TCCC) mimicking human epithelial airway barrier were assessed. Finally, the effect of siRNA-loaded hNPs on ENaC protein expression at 72 hours was evaluated in A549 cells.

Results: Optimized muco-inert hNPs encapsulating model siRNA with high efficiency were produced. The developed hNPs displayed a hydrodynamic diameter of ~ 150 nm, a low polydispersity index, a negative ζ potential close to -25 mV, and a peculiar triphasic siRNA release lasting for 5 days, which slowed down in the presence of PEI. siRNA formulations showed optimal *in vitro* aerosol performance after delivery with a vibrating mesh nebulizer. Furthermore, small-angle X-ray scattering analyses highlighted an excellent stability upon incubation with AM, confirming the potential of hNPs for direct aerosolization on mucus-lined airways. Studies in TCCC confirmed that fluorescent hNPs are internalized inside airway epithelial cells and do not exert any cytotoxic or acute proinflammatory effect. Finally, a prolonged inhibition of ENaC protein expression was observed in A549 cells upon treatment with siRNA-loaded hNPs.

Conclusions: Results demonstrate the great potential of hNPs as carriers for pulmonary delivery of siRNA, prompting toward investigation of their therapeutic effectiveness in severe lung diseases.

Keywords: dipalmitoylphosphatidylcholine, inhalable nanoparticles, poly(ethylenimine), poly(lactic-co-glycolic) acid, siRNA, triple cell coculture

[1]Di.S.T.A.Bi.F., University of Campania "Luigi Vanvitelli," Caserta, Italy.
[2]Laboratory of Drug Delivery, Department of Pharmacy, University of Napoli Federico II, Napoli, Italy.
[3]Adolphe Merkle Institute, University of Fribourg, Fribourg, Switzerland.
[4]Applied Physics, Department of Medical Biotechnology and Translational Medicine, University of Milano, Milano, Italy.
[5]Laboratory of Biochemistry, Department of Pharmacy, University of Napoli Federico II, Napoli, Italy.

Introduction

RNA interference refers to the inhibition of gene expression by small, double-stranded RNA molecules (small interference RNA or siRNA) that direct the mRNA machinery to degrade a specific mRNA. siRNA therapeutics have many advantages in terms of clinical applications, the first of which is their virtual potential to specifically silence any gene underlying more-or-less complex pathologies.[1,2] In particular, severe lung diseases, such as lung cancer or cystic fibrosis (CF), nowadays represent a very important area of application for siRNA-based therapies.[3] Nevertheless, to harness the full potential of the siRNA strategy for severe lung diseases, an appropriately designed delivery system is mandatory.[4,5]

Naked siRNAs have a half-life of less than an hour in human plasma and are often unable to penetrate cell membranes. In fact, cellular uptake and the escape from endolysosomes are critical steps before siRNA reaches the cytoplasm, where its target is located. Conceiving siRNA for local delivery by inhalation, the presence of high mucin, DNA, and actin concentrations, makes airway mucus a very complex barrier to overcome.[4,5] Thus, optimal inhalable formulations are required: (i) to enhance siRNA stability; (ii) to overcome lung cellular and noncellular barriers; and (iii) to increase siRNA availability at the target level.

Amid advanced drug delivery systems, the encapsulation of siRNA into colloidal carriers is considered a very promising formulation approach for inhaled treatment of severe lung diseases.[4,5] In this context, biodegradable poly(lactic-co-glycolic) acid (PLGA) nanoparticles (NPs) are gaining considerable interest since they may provide protection of the therapeutic cargo from enzymatic degradation, prolonged release (i.e., decreased number of administrations), and improved retention in the lungs.[6,7] Nevertheless, particle engineering with excipients aimed to overcome the mucus-lined human lung epithelial barrier is essential.[8,9]

In the attempt to combine the most valuable properties of both lipid and polymeric nanocarriers, hybrid lipid-polymer NPs (hNPs) have recently been proposed.[10,11] Thanks to their ability to form a shell upon the polymer core, lipids may be useful to impart peculiar surface properties to the carrier, likely tuning NP interactions with the lung environment, while enhancing their tolerance in the pulmonary tract.[10] In fact, the use of endogenous phospholipids, such as dipalmitoylphosphatidylcholine (DPPC), can be considered a valid approach to increase NP compatibility with the lung environment. Furthermore, DPPC has been shown to improve the technological features of PLGA particles aimed to nucleic acid delivery to the lung.[12,13]

Along these lines, the aim of this work was to design and optimize hNPs consisting of PLGA and DPPC, introducing PEI as a third component to assist siRNA encapsulation in the hNPs. A preliminary formulation study allowed to select optimized muco-inert DPPC/PLGA and PEI/DPPC/PLGA hNPs displaying optimal *in vitro* aerosol performance. A particular attention was devoted to the characterization of the carrier upon contact with simulated lung fluids through a combination of analytical techniques, that is spectrophotometric assay, dynamic light scattering (DLS), and small-angle X-ray scattering (SAXS).

To allow a proof of principle of RNP potential for siRNA delivery to the lung, selected formulations were loaded with model therapeutic siRNAs of interest for CF therapy, which is a combination of siRNA against the α and β subunits of the sodium transepithelial channel (ENaC). siRNA-loaded hNPs were fully characterized for size, zeta potential, encapsulation efficiency, and *in vitro* release kinetics. A thorough *in vitro* study allowed to assess the fate and the effect of hNPs upon aerosolization on a triple cell co-culture model (TCCC) grown at air–liquid interface (ALI) mimicking the human airway epithelial barrier.[14] Finally, the *in vitro* effects of siRNA-loaded hNPs on the expression of αENaC and βENaC subunits were evaluated on a model human lung epithelial cell line.

Materials and Methods

Materials

Resomer® RG 502H (uncapped PLGA 50:50, inherent viscosity 0.16 0.24 dL/g) was purchased from Evonik Industries AG (Germany). Rhodamine-labeled PLGA was synthesized as previously described.[15] 1,2-dipalmitoyl-sn-glycero-3-phosphocholine (DPPC) was a kind gift of Lipoid GmbH (Switzerland). siGENOME SMARTpool siRNA against α and β subunits of the sodium transepithelial channel (ENaC) (Human SCNN1A and SCNN1B; 19 mer duplexes; Mw = 13.4 kDa) and siGENOME Non-Targeting siRNA Pool were purchased from Dharmacon (GE Healthcare).

Ph.Eur. grade mannitol (Pearlitol® C160) was kindly gifted by Roquette Italia S.p.a. (Italy). Egg yolk emulsion, deoxyribonucleic acid sodium salt from calf thymus (DNA), diethylenetriaminepentaacetic acid (DTPA), phosphate buffer salts, branched polyethylenimine (PEI; 25 kDa), potassium chloride, rhodamine B (Rhod-B), RPMI 1640 amino acid solution, sodium chloride, and mucin from porcine stomach were purchased from Sigma-Aldrich (Missouri). Methylene chloride and ethanol 96% (v/v) were supplied by Carlo Erba (Italy).

Production of DPPC/PLGA hybrid NPs

DPPC/PLGA hNPs were prepared by an emulsion/solvent diffusion technique. Briefly, a water in oil emulsion (w/o) was achieved adding 100 μL of water to 1 mL of methylene chloride containing PLGA (10 mg; 1% w/v) and DPPC at different DPPC/PLGA weight ratios (1:10, 1:20, 1:50, 1:100, and 1:150), under vortex mixing (2400 minutes^{-1}; Heidolph, Germany). When needed, PEI was added to the internal water phase at the theoretical loading of 0.016 mg *per* 100 mg of PLGA. Just after mixing, the w/o emulsion was added to 12.5 mL of ethanol 96% (v/v) under moderate magnetic stirring, leading to immediate nanoparticle precipitation. Then, the formulation was diluted with 12.5 mL of Milli-Q water under stirring for 10 minutes. Afterward, residue organic solvent was removed by rotary evaporation under vacuum at 30°C (Heidolph VV 2000, Germany). hNPs were isolated from the resulting hNP colloidal dispersion (5 mL) by centrifugation at 7000 rcf for 20 minutes at 4°C (Hettich Zentrifugen, Germany) and dispersed in Milli-Q water.

siRNA-loaded hNPs were prepared in optimized formulation conditions at a theoretical loading of 1 nmol/100 mg of PLGA (N/P theoretical ratio of 10 in PEI-modified hNPs) by adding siRNA to the internal water phase.

Fluorescently-labeled hNPs (DPPC/$PLGA_{Rhod}$ and DPPC/$PLGA_{Rhod}$) were prepared using rhodamine-labeled PLGA (PLGA-Rhod) in the organic phase at 10% w/w with respect to the total PLGA amount.

Characterization of DPPC/PLGA hybrid NPs

Size and zeta potential. The hydrodynamic diameter (D_H), the polydispersity index (PI), and the zeta potential (ζ potential) of hNPs were determined by DLS, with a Malvern Zetasizer Nano ZS (Malvern Instruments, United Kingdom). Results are expressed as mean value ± standard deviation (SD) of triplicate measurements in different batches.

siRNA loading inside hNPs. siRNA actual loading was measured indirectly by quantifying the amount of unencapsulated siRNA. Briefly, just after production, hNPs were collected by centrifugation (7000 rcf for 20 minutes at 4°C) and the supernatant was analyzed for siRNA content using Quant-IT™ RiboGreen® reagent (Thermo Fisher Scientific, Massachusetts, Stati Uniti) according to the manufacturer's instructions. Quantitative analysis was performed by spectrofluorimetry at λ_{ex} 480 nm/λ_{em} 520 nm (EnVision® Multilabel Plate Readers, PerkinElmer, Inc.). Results are reported as actual loading (nmol of encapsulated siRNA per mg of yielded hNPs) and encapsulation efficiency (actual loading/theoretical loading × 100) ± SD of values collected from three different batches.

SAXS spectroscopy. Synchrotron SAXS measurements were performed at the ID02 high-brilliance beamline[16] at the ESRF (Grenoble, France), with a beam cross section of 200 × 400 μm and wavelength $\lambda = 0.1$ nm, using two different sample detection distances: 1 and 6 m. The range of investigated momentum transfer, $q = (4\pi/\lambda)\sin(\theta)$, was 0.0116 nm-1 <q <6.43 nm-1, where 2 θ is the scattering angle. All measurements were performed at T = 25°C. Samples were put in plastic capillaries (KI-BEAM, ENKI srl) with 2 mm internal diameter, 0.05 mm wall thickness, and closed with polyethylene caps. Capillaries were then mounted horizontally onto the sample holder. Sample concentration was 10 mg/mL. The exposure time of each measurement was 0.1 seconds, and spectra were checked for radiation damage.

The measured SAXS profiles report the scattered radiation intensity as a function of the momentum transfer, q, where 1 m and 6 m sample-to-detector distance spectra were merged. Solvent subtraction was obtained by measuring water-filled capillaries and empty capillaries.

***In vitro* interaction with mucin.** The light scattering of hNP aqueous dispersions with or without mucin was assessed by spectrophotometry as previously described.[8,17] Briefly, a saturated solution of type II mucin was prepared by centrifugation at 6000 rcf for 20 minutes in a mucin dispersion in water (0.08% w/v) stirred overnight. Then, hNPs were dispersed in the mucin solution at a concentration of 1 mg/mL by vortexing for 1 minute. The light scattering of the mucin/hNPs mixtures was measured by spectrophotometric analysis at 650 nm at time 0 and after incubation for 30 and 60 minutes at room temperature. Reference absorbances of mucin and 1 mg/mL hNP dispersions in water were also evaluated. Experiments were run in triplicate and results are expressed as absorbance at 650 nm ± SD over time.

The interactions of hNPs with mucin were further investigated by DLS as previously reported.[9] Briefly, the hNP dispersions in mucin were examined with the Malvern Zetasizer Nano ZS (Malvern Instruments, United Kingdom). Experiments were run in triplicate and results are reported as representative size distribution by intensity of hNPs in mucin versus hNPs in water. The size distribution profile of the mucin solution was also recorded as control.

Particle stability in artificial mucus. To assess the stability of siRNA-loaded hNPs and their ability to diffuse inside airway mucus, SAXS analyses were performed on hNP dispersions in the presence of artificial mucus (AM). As previously reported,[8] AM was prepared by adding 25 μL of sterile egg yolk emulsion, 25 mg of mucin, 20 mg of DNA, 30 μL of aqueous DTPA (1 mg/mL), 25 mg NaCl, 11 mg KCl, and 100 μL of RPMI 1640 to 5 mL of water. The dispersion was stirred until a homogenous mixture was obtained. For stability studies, aqueous dispersions of siRNA-loaded hNPs (10 mg/mL) were mixed with AM in a 1:3 volume ratio for a total 40 μL sample volume. After a 1-hour equilibration time, SAXS was performed as described above. Particle structure after a 12-hour incubation with AM was verified by repeated SAXS measurements.

***In vitro* release kinetics of siRNA.** siRNA-loaded hNPs were characterized for *in vitro* siRNA release kinetics in phosphate buffer (120 mM NaCl, 2.7 mM KCl, and 10 mM Na2HPO4) at pH 7.2 (phosphate-buffered saline [PBS]). Release studies were performed upon dilution of hNP dispersions in PBS to a theoretical siRNA concentration of 0.2 nmol/mL. hNP dispersions were incubated in a horizontal shaking water bath at 37°C (ShakeTemp SW 22, Julabo, Italy). At scheduled time intervals, samples were centrifuged at 7000 rcf for 20 minutes at 4°C to isolate hNPs and the release medium was withdrawn and analyzed for siRNA content by spectrofluorimetric analysis as described for actual loading. The medium was replaced by the same amount of fresh PBS. Experiments were carried out in triplicate and results expressed as the percentage of siRNA released ± SD.

***In Vitro* aerosol performance.** The aerosolization properties of fluorescently-labeled DPPC/$PLGA_{Rhod}$ and PEI/DPPC/$PLGA_{Rhod}$ hNP dispersions were investigated *in vitro* after delivery from the Aeroneb® Go nebulizer (Aerogen Ltd., Ireland) by a Next Generation Impactor (NGI) (Copley Scientific, United Kingdom) according to the Comité Européen de Normalization (CEN) standard methodology for nebulizer systems with sampling at 15 L/minutes and insertion of a filter in micro-orifice collector (MOC).[18] Briefly, 1 mL of hNP dispersion was transferred to the reservoir of the nebulizer, which was connected to the induction port of the NGI. The nebulizer was operated at 15 L/minutes, and the aerosol was drawn through the impactor for 5 minutes, until dryness.

The amount of fluorescent hNPs remaining inside the nebulizer chamber, deposited on the seven NGI collection cups, and in the induction port was quantitatively recovered in NaOH 0.5 M. After stirring at room temperature for 1 hour, the amount of fluorescent hNPs in the resulting solutions was determined by spectrofluorimetric analysis at λ_{ex}

553 nm/λ_{em} 577 nm (GloMax® Explorer, Promega, Italy) as previously reported.[8] Calibration curves were derived by analyzing serial dilutions of DPPC/$PLGA_{Rhod}$ or PEI/DPPC/$PLGA_{Rhod}$ standard solutions prepared from a stock of hNPs degraded in NaOH 0.5 M. The linearity of the response was verified over the concentration range 2–200 μg/mL ($r^2 \geq 0.999$). Each experiment was run in triplicate.

The emitted dose (ED) was measured as the difference between the total amount of hNPs initially placed and the amount remaining in the nebulizer chamber. Upon emission, the experimental mass median aerodynamic diameter ($MMAD_{exp}$) and the geometric SD (GSD) were calculated according to the European Pharmacopoeia, deriving a plot of cumulative mass of particle retained in each collection cup (expressed as percent of total mass recovered in the impactor) versus the cutoff diameter of the respective stage.

The fine particle fraction (FPF) was calculated taking into account the amount of hNPs deposited in stages 3–7 ($MMAD_{exp}$ <5.39 μm) compared to the initial amount loaded into the nebulizer chamber, while the respirable fraction (RF) referred to the total amount recovered from the NGI.

In vitro *studies on airway triple cell cocultures*

All *in vitro* exposure experiments were conducted with a three-dimensional TCCC mimicking the human epithelial airway barrier comprising human bronchial epithelial cells (16HBE14o-), human blood monocyte-derived macrophages (MDM), and dendritic cells (MDDC).[14]

16HBE14o- cell cultures. 16HBE14o- cells were kindly provided by Dieter Gruenert (passage number P2.54; University California, San Francisco, CA). Cells were maintained in minimum essential media 1× (with Earle's Salts, 25 mM HEPES and without L-glutamine; Gibco BRL, Thermo Fisher Scientific), supplemented with 1% L-glutamine, 1% penicillin/streptomycin, and 10% fetal calf serum.

For experimental cultures, cells were seeded at a density of 0.5×10^6 cells/insert on transparent BD Falcon (Corning) cell culture inserts (surface area of 0.9 cm^2, pores with 3.0 μm diameter, and PET membranes for 12-well plates). The cell culture inserts were pretreated with 150 μL of a fibronectin coating solution containing 0.1 mg/mL bovine serum albumin (Sigma-Aldrich), 1% Type I bovine collagen (BD Biosciences, Becton Dickinson, New Jersey), and 1% human fibronectin (BD Biosciences, Becton Dickinson) in the LHC Basal Medium (Sigma-Aldrich). Inserts were placed in BD Falcon tissue culture plates (12-well plates) with 0.5 mL medium in the upper and 1.5 mL in the lower chamber. The cells were kept at 37°C in 5% CO_2 humidified atmosphere for 7 days (medium changed after 3–4 days).

TCCC system. To produce the TCCC *in vitro* model, 16HBE14o- cell cultures were supplemented on the apical side with MDM and on the basolateral side with MDDC derived from human blood as previously reported.[14,19] Briefly, 16HBE14o- cells were cultured as described above. At 5 days, the medium was removed from the upper and lower chamber, the inserts turned upside down, and the bottom was abraded carefully with a cell scraper. The inserts were then incubated with 65 μL medium containing 83×10^4 MDDC/mL on the basal side for 2 hours. Afterward, the inserts were turned around again and placed in BD Falcon (Corning) tissue culture plates (12-well plates). In the lower chamber, 1.5 mL of medium, and at the apical side of the TCCC, 500 μL medium containing 2.5×10^4 MDM/mL were added. The complete TCCC systems were kept with 1.5 mL of medium in the lower chamber and 0.5 mL in the upper chamber at 37°C in 5% CO_2 humidified atmosphere for 24 hours.

To establish the ALI, the medium in the upper chamber of the TCCC systems was removed 24 hours before exposure in the Vitrocell® Cloud, while the medium in the lower chamber was replaced by 0.6 mL of fresh medium.

***In vitro* TCCC exposure to aerosolized NPs.** Cell exposure to hNPs at ALI was carried out with the Vitrocell Cloud system (Vitrocell Systems GmbH, Germany). Briefly, the Vitrocell Cloud consists of three main components: a nebulizer, an exposure chamber, and a flow system, with an incubation chamber providing suitable temperature and humidity cell culture conditions. The aerosol is generated into the exposure chamber by a perforated vibrating membrane nebulizer (AeronebPro, with a span of 2.5–6.0 μm volume mean diameter). Before each experiment, freeze-dried hNPs were dispersed in 0.5 mM sodium chloride.

For TCCC exposure to low hNP concentrations, 200 μL of a 0.5 mg/mL hNP dispersion was aerosolized (0.1 mg of hNPs). For high hNP concentrations, TCCC were exposed to further 400 μL (2 × 200 μL) of a 0.9 mg/mL hNP dispersion (0.5 mg of hNPs). TCCC exposed to 0.5 mM sodium chloride and mannitol aqueous solutions was used as controls. Following the exposure in the chamber (10 and 30 minutes for 0.1 and 0.5 mg of hNPs, respectively), the inserts were immediately placed in new BD Falcon 12- well tissue culture plates containing 0.6 mL of fresh medium for cell uptake studies, cytotoxicity assay, and tumor necrosis factor alpha (TNF-α) release. The morphology of hNPs was analyzed by transmission electron microscopy (TEM) before nebulization and after exposing a 400 mesh copper film grid to nebulized hNPs. The analysis was performed with a FEI Tecnai spirit TEM at 120 kV and images were acquired with a Veleta CCD camera (2048 × 2048 pixels).

Nanoparticle deposition efficiency. The amount of hNPs deposited upon nebulization inside the Vitrocell Cloud was assessed. To this purpose, glass coverslips (24 × 24 mm) were placed onto the compartments for cell culture inserts and exposed to different amounts of aerosolized rhodamine-labeled DPPC/$PLGA_{Rhod}$ and PEI/DPPC/$PLGA_{Rhod}$ hNPs. After the exposure, coverslips were removed and rinsed with NaOH 0.5 M (500 μL). After stirring at room temperature for 1 hour, the amount of fluorescent hNPs in the solutions was quantified by spectrofluorimetric analysis as described for *in vitro* aerosol performance. Results are reported as μg of hNPs deposited *per* $cm^2 \pm$ SD of values collected from triplicate analyses.

Cell uptake studies. The TCCC was exposed to different amounts of aerosolized rhodamine-labeled DPPC/$PLGA_{Rhod}$ and PEI/DPPC/$PLGA_{Rhod}$ hNPs. After 24 hours postexposure, TCCC were fixed for 15 minutes with 3% paraformaldehyde in PBS at room temperature and cells were washed thrice in PBS. The F-actin cytoskeleton and the DNA of all cells were stained with phalloidin (ALEXA 488) (Molecular Probes, Life Technologies Europe B.V., Switzerland) and

4′,6- diamidin-2-phenylindol (DAPI) (1 μg/mL) in a 1:100 and 1:50 dilution in 0.3% Triton X-100 in PBS, respectively. For microscopy, membranes were embedded in Glycergel (DAKO Schweiz AG, Baar, Switzerland). Sample analysis was performed with an inverted Zeiss confocal laser scanning microscope 710 (LSM, Axio Observer.Z1, Zeiss, Germany). Representative images (z-stacks) were recorded at three independent fields of view for each sample. Image processing was achieved using the 3D reconstruction software Imaris (Bitplane AG, Switzerland).

Cytotoxicity assay. The TCCC was exposed to different amounts of aerosolized siRNA-DPPC/PLGA and siRNA-PEI/DPPC/PLGA, and corresponding empty hNPs. After 24 hours postexposure at 37°C, lactate dehydrogenase (LDH) release by the TCCC, indicative of cell membrane damage, was assessed by the LDH cytotoxicity detection kit (Roche Applied Science, Germany) according to the manufacturer's guidelines. The test was performed in triplicates and evaluated in comparison to the negative controls, which are TCCC exposed to aqueous solutions of 0.5 mM sodium chloride or mannitol at the same concentrations of hNP dispersions. As a positive control, TCCC were treated with 100 μL of 0.2% Triton X-100 in PBS on the apical side and incubated for 24 hours at 37°C and 5% CO_2.

Tumor necrosis factor-α release. The potential proinflammatory response was also investigated after 24 hours postexposure to hNPs by quantifying the release of TNF-α using an ELISA kit (R&D Systems) according to the manufacturer's protocol.

In vitro *gene silencing effect*

Cell cytotoxicity. A549 cells were seeded onto 96-well plates (5×10^4 cells/well) and incubated with hNPs for 24 and 48–72 hours. Then, cell viability was evaluated by MTT assay as previously reported.[20a]

Cell culture, transfection, and treatment. Human alveolar basal epithelial cell line (A549) was cultured in Dulbecco's modified Eagle's medium supplemented with 10% heat-inactivated fetal bovine serum (Microtech), 1.5 mM L-glutamine, 100 units/mL penicillin, and 100 μg/mL streptomycin under humidified atmosphere of 5% CO_2 at 37°C. siRNA transfections and treatments were performed as previously described.[20b]

Western blotting. Total proteins (75 μg) were extracted from the cells, separated on 10% sodium dodecyl sulfate–polyacrylamide gel electrophoresis and electrotransferred on polyvinylidene fluoride (PVDF) as previously described.[21] Then, the membrane was incubated for 2 hours with 5% nonfat milk to block nonspecific binding sites and incubated 2 hours at room temperature with the following antibodies: anti-βENaC (Santa Cruz Biotechnology), anti-SCNN1A (Proteintech Europe), and anti-β-actin (Santa Cruz Biotechnology). Densitometric analysis was carried out using ImageJ software (Image 1.49v, available on: http://imagej.nih.gov/ij, National Institutes of Health, Bethesda, MD).

Data analysis

Cell studies were performed in triplicate and results are expressed as mean value ± standard error mean ($n=3$). The significance of differences was determined with the software Kaleida graph using one-way analysis of variance followed by Bonferroni *post-hoc* test. A p-value <0.05 was considered significant.

Results

Development studies of DPPC/PLGA hNPs for siRNA loading

In-depth formulation studies were performed on empty hNPs to establish the optimal ratio between the selected components, that is, PLGA, DPPC, and PEI. Overall hNP properties are reported in Table 1.

Independent of the amount of DPPC added to the organic phase and the presence of PEI in the internal water phase, the adopted formulation conditions lead to the formation of hNPs with D_H ranging between ~135 and ~169 nm, low PI (<0.130), and negative ζ potentials (between −16 and −30 mV). Nevertheless, in each case, a flocculation of the exceeding amount of the lipid component was apparent after rotary evaporation of the diffusion solvent under vacuum.

This phenomenon was particularly evident when high amounts of DPPC were added to the formulation (i.e., DPPC/

Table 1. Composition, Size, Polydispersity Index, and Zeta Potential of Empty DPPC/PLGA and PEI/DPPC/PLGA Hybrid Lipid-Polymer Nanoparticles

Formulation	*PEI theoretical loading (mg/100 mg of PLGA)*	*DPPC/PLGA ratio (w/w)*	*D_H (nm ± SD)*	*PI (mean ± SD)*	*ζ potential (mV ± SD)*
DPPC/PLGA10	—	1:10	151.3 ± 21.3	0.127 ± 0.079	−25.3 ± 0.5
DPPC/PLGA 20	—	1:20	149.7 ± 2.1	0.083 ± 0.006	−23.2 ± 2.4
DPPC/PLGA 50	—	1:50	135.4 ± 17.2	0.088 ± 0.008	−24.3 ± 6.0
DPPC/PLGA 100	—	1:100	158.9 ± 7.1	0.082 ± 0.004	−28.4 ± 2.9
DPPC/PLGA 150	—	1:150	168.6 ± 7.1	0.124 ± 0.094	−15.7 ± 1.3
PEI/DPPC/PLGA 10	0.016	1:10	166.5 ± 13.9	0.128 ± 0.093	−26.1 ± 0.5
PEI/DPPC/PLGA 20	0.016	1:20	165.4 ± 9.1	0.102 ± 0.006	−31.7 ± 1.2
PEI/DPPC/PLGA 50	0.016	1:50	162.3 ± 13.9	0.124 ± 0.041	−28.0 ± 0.7
PEI/DPPC/PLGA 100	0.016	1:100	150.9 ± 30.4	0.106 ± 0.027	−28.0 ± 0.3
PEI/DPPC/PLGA 150	0.016	1:150	146.4 ± 0.3	0.123 ± 0.027	−22.2 ± 2.7

PI, polydispersity index; SD, standard deviation.

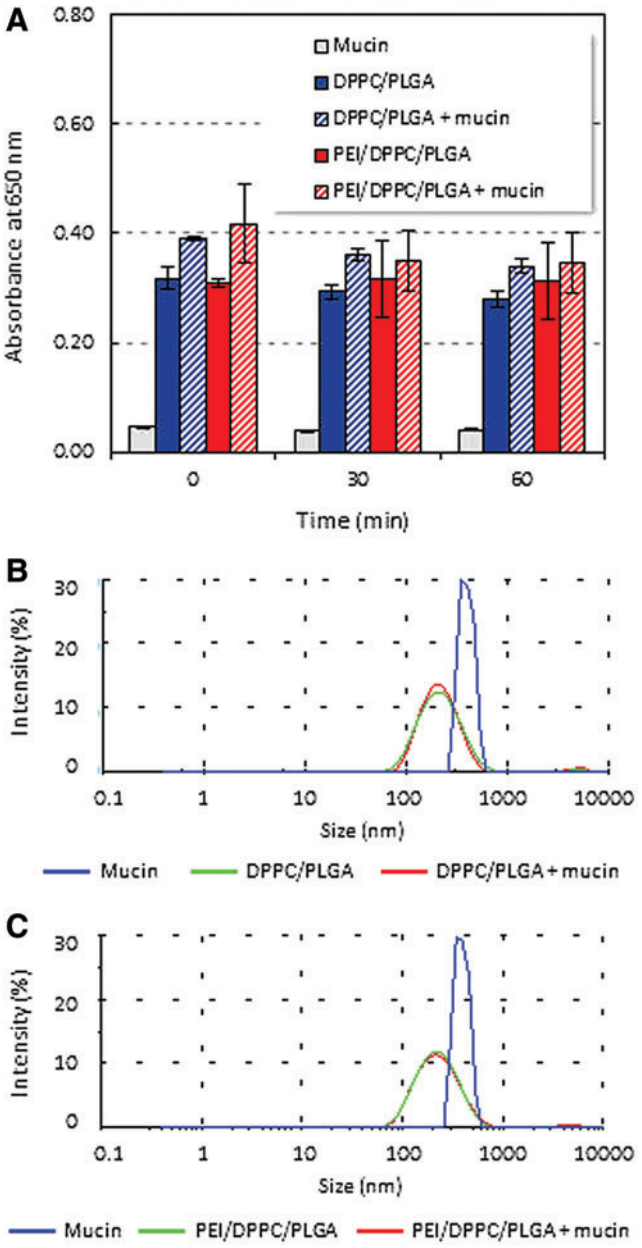

FIG. 1. *In vitro* assessment of mucin interactions with optimized empty DPPC/PLGA and PEI/DPPC/PLGA hNPs. **(A)** Scattering at 650 nm of hNPs in mucin (1 mg/mL) over time. The absorbance at 650 nm of mucin and hNP dispersions in water is reported as control. **(B–C)** Size distribution by intensity of hNP dispersions in water or a saturated mucin solution evaluated by DLS. The size distribution profile of mucin in water is reported as control **(B** DPPC/PLGA hNPs and **C** PEI/DPPC/PLGA). hNPs, hybrid lipid-polymer nanoparticles. Color images available online at www.liebertpub.com/jamp

PLGA 1:10 w/w), but it was limited up to a theoretical DPPC/PLGA ratio of 1:20. Thus, this last ratio was selected for further studies to maximize the amount of DPPC associated to the NPs, while limiting flocculation. The corresponding formulations, from here on, are named DPPC/PLGA and PEI/DPPC/PLGA.

Mucin/nanoparticle interaction studies were performed by measuring the absorbance at 650 nm of DPPC/PLGA and PEI/DPPC/PLGA hNPs in mucin over time (Fig. 1A). While the absorbance of the reference mucin dispersion was close to zero, higher values of absorbance were observed at each time point upon addition of hNP dispersions. Nevertheless, no significant differences were observed between absorbance of hNPs dispersed in water or mucin (Fig. 1A). The interactions between mucin and either DPPC/PLGA or PEI/DPPC/PLGA hNP were analyzed also by DLS (Fig. 1B, C, respectively).

The combined particle size distribution for the various replicates shows no change in the position and intensity of the peak. In line with previous studies,[9] the apparent dimension of bare PLGA is significantly shifted to larger sizes upon addition of mucin, reflecting strong mucin/NP hydrophobic interactions, which likely provide a basis for mucoadhesive NPs (Supplementary Fig. S1A; Supplementary Data are available online at www.liebertpub.com/jamp). A similar behavior was observed for bare PEI-PLGA NPs (Supplementary Fig. S1B).

Characterization of siRNA-loaded DPPC/PLGA hNPs

A model siRNA against ENaC was entrapped in DPPC/PLGA and PEI/DPPC/PLGA formulations at the theoretical loading of 1 nmol/100 mg of PLGA. The addition of siRNA inside the formulation did not result in significant changes of hNP size and PI (Table 2) compared to empty hNPs (Table 1). siRNA-loaded hNPs with a D_H around 140 nm (141 and 142 nm for siRNA-DPPC/PLGA and siRNA-PEI/DPPC/PLGA, respectively) and low PI were produced with good yields (52% and 53% for siRNA-DPPC/PLGA and siRNA-PEI/DPPC/PLGA, respectively). siRNA was effectively incorporated inside DPPC/PLGA hNPs with a mean encapsulation efficiency of 75%. The addition of PEI inside the formulation allowed to reach an excellent encapsulation efficiency of 96%, thus increasing siRNA actual loading from 1.35 to 1.74 nmol per 100 mg of hNPs.

Results of *in vitro* release studies performed at physiological pH and temperature (pH 7.2 and 37°C) are reported in Figure 2 as percentage of siRNA released over time.

Both siRNA-DPPC/PLGA and siRNA-PEI/DPPC/PLGA hNPs displayed a typical triphasic release profile, characterized by an initial burst, with more than 50% of siRNA released in the first hours, followed by a slow release phase lasting a couple of days and a final fast release time period after 4–5 days. Although, both formulations show similar release profile, siRNA/

TABLE 2. PROPERTIES OF siRNA-LOADED HYBRID LIPID-POLYMER NANOPARTICLES

	siRNA-DPPC/PLGA	*siRNA-PEI/DPPC/PLGA*
D_H (nm ± SD)	141 ± 0.50	142 ± 1.8
PI (mean ± SD)	0.120 ± 0.018	0.114 ± 0.0050
ζ potential (mV ± SD)	−29.1 ± 1.6	−29.9 ± 1.4
Yield of production (% ± SD)	52.0 ± 8.9	53.4 ± 2.5
siRNA actual loading[a] (% ± SD)	1.35 ± 0.02	1.74 ± 0.04
Encapsulation efficiency (% ± SD)	74.8 ± 1.5	95.9 ± 2.2

[a]siRNA loading was expressed as nmol of encapsulated siRNA *per* 100 mg of hNPs. siRNA theoretical loading was 1 nmol/100 mg of hNPs.

hNPs, hybrid lipid-polymer nanoparticles.

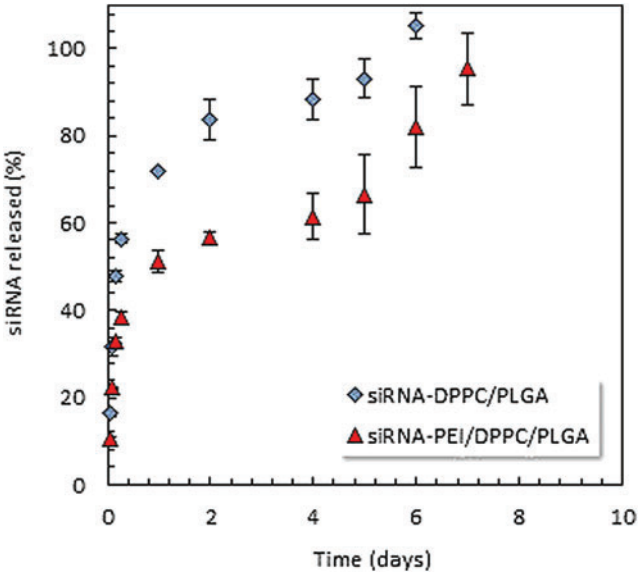

FIG. 2. *In vitro* release kinetics of siRNA from hNPs in PBS at pH 7.2. Data are expressed as siRNA released (%) ± SD ($n = 3$). PBS, phosphate-buffered saline; SD, standard deviation. Color images available online at www.liebertpub.com/jamp

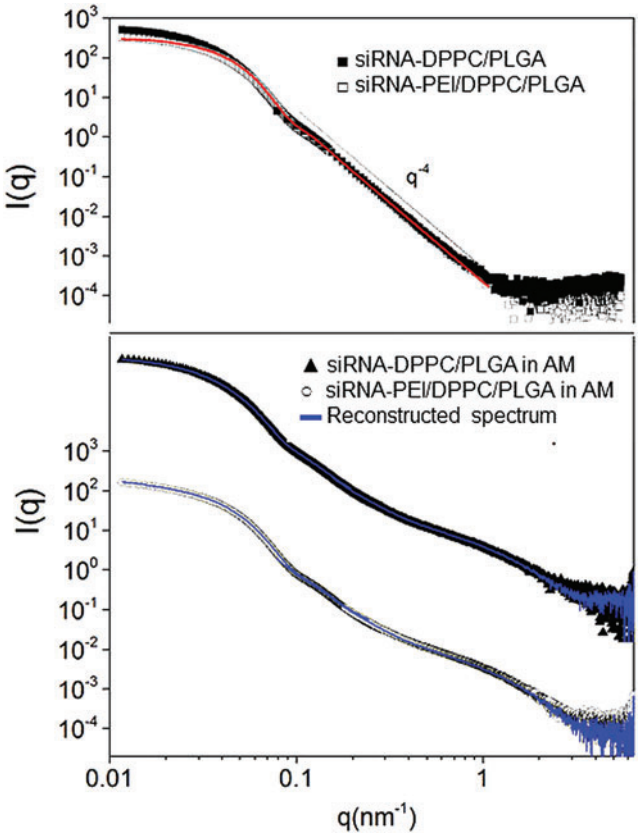

FIG. 3. Small-angle X-ray scattering spectra of siRNA-loaded hNPs. Top panel: siRNA-DPPC/PLGA (full dots) and siRNA-PEI/DPPC/PLGA (empty dots) in water. The red line is the representative fitting of the siRNA-PEI/DPPC/PLGA data with the form factor of a polydisperse sphere (red line). Bottom panel: siRNA-DPPC/PLGA (top) and siRNA-PEI/DPPC/PLGA (bottom) after 12 hours of incubation with artificial mucus (AM) (empty dots) versus a reconstructed spectrum obtained by summing up AM and naked hNP spectra (blue line). siRNA-DPPC/PLGA spectrum is stacked for clarity. Color images available online at www.liebertpub.com/jamp

DPPC/PLGA hNPs provided a significantly more rapid release compared to siRNA-PEI/DPPC/PLGA hNPs. Nevertheless, both hNP formulations sustained siRNA release for 1 week.

The I(q) SAXS spectra of siRNA-DPPC/PLGA and siRNA-PEI/DPPC/PLGA hNPs are reported in Figure 3 (Top panel). A low q region affected by the finite size of the particle in the range of the 100 nm distances can be identified. At higher q, an extended region with q-4 slope shows up, which identifies a sharp solvent–particle interface and a smooth particle surface. Giunier analysis[22] in the interval $0.0116\ nm^{-1} < q < 0.0246\ nm^{-1}$ gives gyration radii $Rg = 53 \pm 0.5$ nm and $Rg = 52 \pm 0.6$ nm for siRNA-DPPC/PLGA and siRNA-PEI/DPPC/PLGA hNPs, respectively. If modeled as spheres, this corresponds to particle radii of 68 and 67 nm, in good agreement with hydrodynamic radii (Table 2). The best fit of I(q) is obtained by applying the form factor of a distribution of polydispersed spheres with a number-averaged mean radius of 45 ± 9 nm for siRNA-DPPC/PLGA and 42 ± 11 nm for siRNA-PEI/DPPC/PLGA hNPs. The fits are shown in Figure 3 (red lines).

The phospholipid component is possibly coating the PLGA particle, without forming a bilayer envelope. A comparison of the spectra of bare PLGA NPs and DPPC/PLGA hNPs is reported in Supplementary Figure S2 to better illustrate this point. We underline that PEI and siRNA contents are actually of the order of μg over 10 mg of particles, so that scattering contribution from those components are not detectable.

Applying SAXS analysis, the stability of hNPs in mucus was studied during 12 hours after mixing AM with aqueous dispersions of hNPs in a 3:1 volume ratio. The scattering spectra obtained after equilibration over 12 hours are reported in Figure 3 (Bottom panel). Of note, the obtained spectrum is consistent with the sum of the naked particle spectrum and the mucus spectrum that give the reconstructed line shown in the figure (blue line).

In vitro aerosol performance of the optimized hNP formulations was first assessed through NGI. To easily quantify the amount of hNPs deposited in each cup, blank fluorescent DPPC/PLGA$_{Rhod}$ and PEI/DPPC/PLGA$_{Rhod}$ hNPs were used (Fig. 4). In fact, neither the presence of siRNA nor the addition of PLGA-Rhod affected hNP size and surface properties, which are crucial for aerosolization.

According to the new regulatory guidance, both USP and Ph.Eur. recognize the suitability of the NGI for nebulizer characterization when used at 15 L/min excluding the pre-separator and placing an internal filter below the MOC.[18] In this configuration, the seven NGI stages produce cutoff diameters in the range 14.1–0.98 μm, while the last five stages have cutoff diameters between 5.39 and 0.98 μm. Figure 4A describes the cumulative droplet size distribution of the hNP dose emitted after aerosolization from an Aeroneb Go vibrating-mesh nebulizer. In both cases, the best fit line was from logarithmic linear regression ($r^2 > 0.96$). The deposition patterns of DPPC/PLGA$_{Rhod}$ and PEI/DPPC/PLGA$_{Rhod}$ throughout the NGI cups are shown in Figure 4B. In both cases, less than 1.5% of the ED of hNPs was deposited in the throat, with 65%–75% of the ED recovered from Cups 3–7 ($MMAD_{exp} < 5.39\ \mu$m).

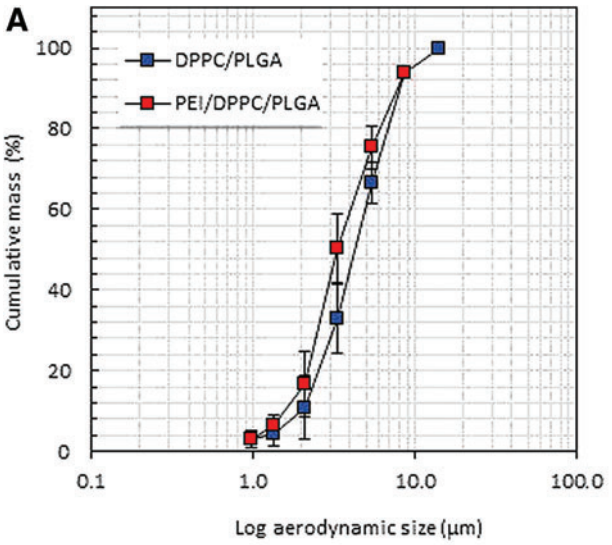

C

	DPPC/PLGA	PEI/DPPC/PLGA
$MMAD_{exp}$ (μm ± SD)	3.96 ± 0.34	3.52 ± 0.20
GSD (± SD)	2.25 ± 0.05	2.26 ± 0.09
FPF (% ± SD)	17.5 ± 2.0	21.5 ± 3.3
RF (% ± SD)	66.4 ± 3.7	73.2 ± 6.9

FIG. 4. *In vitro* aerosol performance of DPPC/PLGA and PEI/DPPC/PLGA hNPs upon delivery through the Aeroneb® Go nebulizer. **(A)** Cumulative mass recovered as a function of the cutoff diameter of the NGI stages; **(B)** NGI deposition pattern; **(C)** fine particle characteristics of the aerosol cloud. Data are presented as mean ± SD ($n = 3$). NGI, Next Generation Impactor. Color images available online at www.liebertpub.com/jamp

Nevertheless, while $DPPC/PLGA_{Rhod}$ formulation showed a peak at 5.39 μm, the highest percent of $PEI/DPPC/PLGA_{Rhod}$ was recovered from cup with a cutoff diameter of 3.3 μm. As a consequence, by the same value of GSD, $PEI/DPPC/PLGA_{Rhod}$ hNPs displayed a lower $MMAD_{exp}$ and, consequently, higher FPF and RF values compared to $DPPC/PLGA_{Rhod}$ (Fig. 4C).

In vitro *aerosolization of hNPs on TCCC*

The ability of aerosolized hNPs to penetrate airway epithelial barrier was probed *in vitro* on TCCC. The experiments were carried out on fresh dispersions of freeze-dried hNPs (1:25 hNP/mannitol weight ratio) in 0.5 mM NaCl for ideal nebulization. Mannitol was added to the hNPs as cryoprotectant to avoid common hNP aggregation in a collapsed cake.[23] In fact, it induced the lowest variation of D_H and PI with respect to the control, and no difference was observed when changing the hNP/cryoprotectant ratio (Supplementary Table S1 and Supplementary Fig. S3). Furthermore, mannitol could also work facilitating hNP transport through mucus, and in so doing siRNA diffusion, due to its established ability to improve fluidity of mucus.[24]

The stability of hNPs during the nebulization process was confirmed by transmission electron microscopy (TEM) analysis of freeze-dried siRNA-loaded hNPs in the presence of mannitol (1:25 NP/mannitol ratio) before and after nebulization in the Vitrocell Cloud (Fig. 5). TEM images suggest a potential core-shell structure for both siRNA-DPPC/PLGA and siRNA-PEI/DPPC/PLGA, which was retained after the nebulization process, which did not cause any apparent modification of the hNP structure or hNP aggregation for each tested concentration.

The deposition efficiency was also evaluated for both tested formulations, highlighting in each case a homogeneous distribution of the hNPs on the coverslips inside the exposure chamber (Supplementary Fig. S4) and a direct correlation between the delivered and deposited doses of hNPs. In particular, 0.0051 ± 0.0018 and 0.0127 ± 0.0058 $\mu g/cm^2$ of hNPs were deposited on coverslips after nebulization of $DPPC/PLGA_{Rhod}$ dispersions at low and high concentrations, respectively.

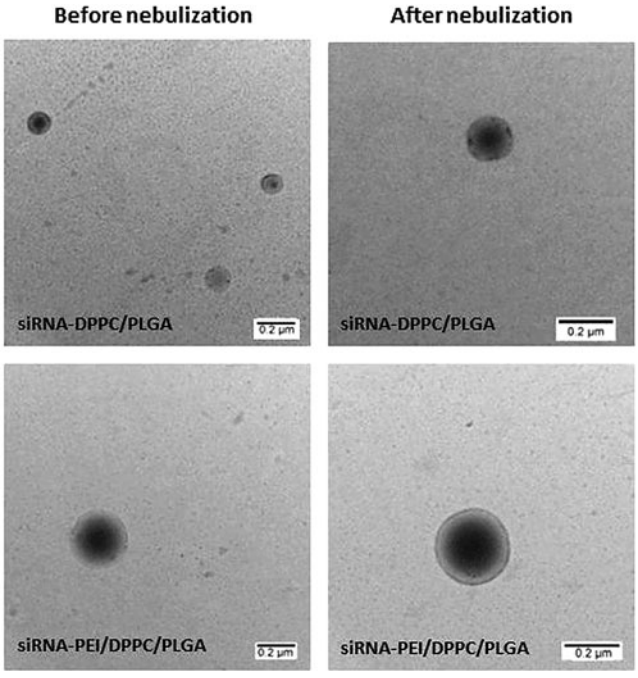

FIG. 5. Transmission electron microscopy (TEM) images of reconstituted freeze-dried siRNA-loaded hNPs (siRNA-DPPC/PLGA and siRNA-PEI/DPPC/PLGA) before and after nebulization. Scale bar is 0.2 μm. Field is representative of the sample.

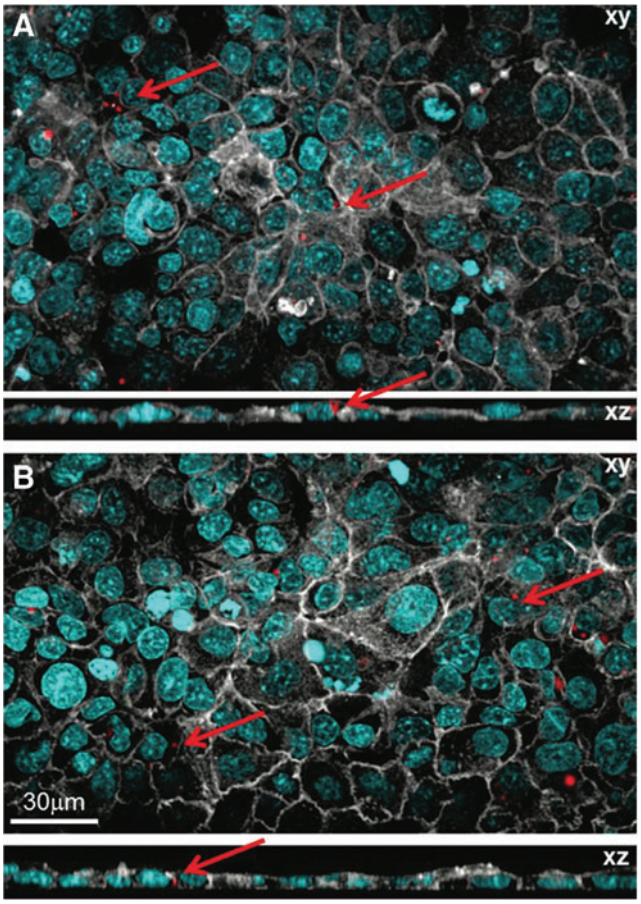

FIG. 6. CLSM images of TCCC after 24 hours postexposure to 0.5 mg of fluorescently labeled DPPC/PLGA$_{Rhod}$ **(A)** and PEI/DPPC/PLGA$_{Rhod}$ **(B)** hNPs. Red color corresponds to the hNPs, white color to cytoskeletal F-actin, and cyan color to nulcei. The arrows show hNPs engulfed by the cells. TCCC, triple cell coculture model. Color images available online at www.liebertpub.com/jamp

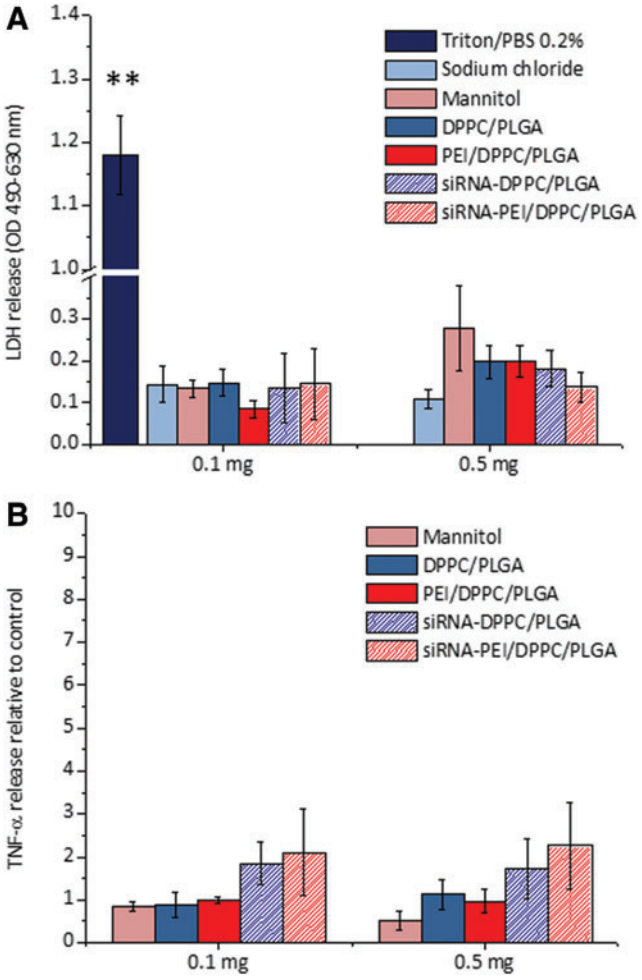

FIG. 7. LDH release **(A)** and TNF-α secretion **(B)** of TCCC after 24 hours postexposure to different theoretical amounts (0.1 and 0.5 mg) of aerosolized empty or siRNA-loaded hNPs. Sodium chloride was used as negative control. Mannitol aqueous solutions at the same volume and concentrations used for hNP samples were also aerosolized for comparison. Triton 0.2% (w/v) in PBS was used as positive control in LDH release **(A)**. LDH data are presented as mean optical density (OD) values ± SEM of samples diluted 1:10 v/v in cell culture medium ($n=3$) (**$p<0.001$). TNF-α data are presented as the mean fold increase of samples relative to the negative control (i.e., sodium chloride) ± SEM ($n=3$). LDH, lactate dehydrogenase; SEM, standard error mean; TNF-α, tumor necrosis factor alpha. Color images available online at www.liebertpub.com/jamp

Meanwhile, likely, as a consequence of the good aerosolization properties of PEI-containing formulations, 0.0137 ± 0.0032 and 0.0334 ± 0.0069 $\mu g/cm^2$ of hNPs were recovered from coverslips after nebulization of low and high concentrations of PEI/DPPC/PLGA$_{Rhod}$ hNPs, respectively.

Fate and cytotoxicity of aerosolized hNPs in TCCC

To study the cell uptake, fluorescently labeled hNPs were aerosolized on TCCC. After 24 hours postexposure to hNPs, TCCC were visualized by CLSM (Fig. 6). Results indicate that both DPPC/PLGA$_{Rhod}$ and PEI/DPPC/PLGA$_{Rhod}$ hNPs (labeled in red) can effectively penetrate into cells and are localized intracellularly.

At the tested concentrations, the developed hNPs displayed no significant cytotoxicity compared to both sodium chloride and mannitol solutions aerosolized at the same concentrations of the samples ($p>0.5$) (Fig. 7A). On the other hand, a significant cytotoxic effect was observed when the cocultures were incubated with Triton-X as positive control ($p<0.001$ versus DPPC/PLGA$_{Rhod}$ and PEI/DPPC/PLGA$_{Rhod}$). These findings were confirmed by CLSM analysis of all treated samples, since no alteration of cell morphology occurred after TCCC exposure to hNPs compared to the negative control (Supplementary Fig. S5).

The potential proinflammatory effect of aerosolized empty and siRNA-loaded hNPs on TCCC was also investigated by determining TNF-α secretion 24 hours postexposure (Fig. 7B). Of note, exposure to mannitol and empty hNPs, at both low and high concentration, caused a less than onefold increase of TNF-α release to the TCCC exposed to 0.5 mM aqueous sodium chloride. As for siRNA-loaded hNPs, we can see at all concentrations tested a higher production of TNF-α in comparison to negative control, although values were not significantly different from the mannitol control.

In vitro *silencing effect of siRNA-loaded hNPs*

Once proven that the developed hNPs are able to overcome the lung barriers and reach the target cells, we further evaluated the effect of siRNA-loaded hNPs on gene silencing efficiency in a human lung epithelial cell line, that is A549 cells. Preliminary cytotoxicity studies showed that both DPPC/PLGA and PEI/DPPC/PLGA hNPs exhibited a safe profile toward A549 cells in a wide range of concentrations (from 0.2 to 2 mg/mL) up to 72 hours of incubation (Supplementary Fig. S6). Nevertheless, to determine the amount of siRNA-loaded hNPs necessary to obtain an efficient gene depletion, dose–response studies were further performed by transiently transfecting A549 cells with increasing concentrations of siRNA pool by using lipofectamine. Results showed a specific and dose-dependent silencing of both αENaC and βENaC subunits (Supplementary Fig. S7). In particular, while nontargeting siRNA pool at 20 nM did not exert any effect on the levels of αENaC and βENaC subunits (data not shown), siRNA pool against ENaC resulted in robust protein knockdown at 24 hours (about 50% and 60% of gene depletion for αENaC and βENaC, respectively). This siRNA concentration was thus selected for *in vitro* gene silencing studies with siRNA-loaded hNPs. We found that siRNA pool slowly released from hNPs resulted in efficient knockdown of both αENaC and βENaC subunit proteins up to 72 hours (Fig. 8). Western blots confirmed that protein expression was significantly reduced by more than 60% and 40% for αENaC and βENaC, respectively, by siRNA-DPPC/PLGA hNPs compared to control (untreated cells). Of note, the addition of PEI inside the formulation increased the silencing efficiency of siRNA-loaded hNPs by a further significant 10% compared to siRNA-DPPC/PLGA hNPs. The same amount of blank DPPC/PLGA and PEI/DPPC/PLGA hNPs did not affect the levels of ENaC subunits (data not shown).

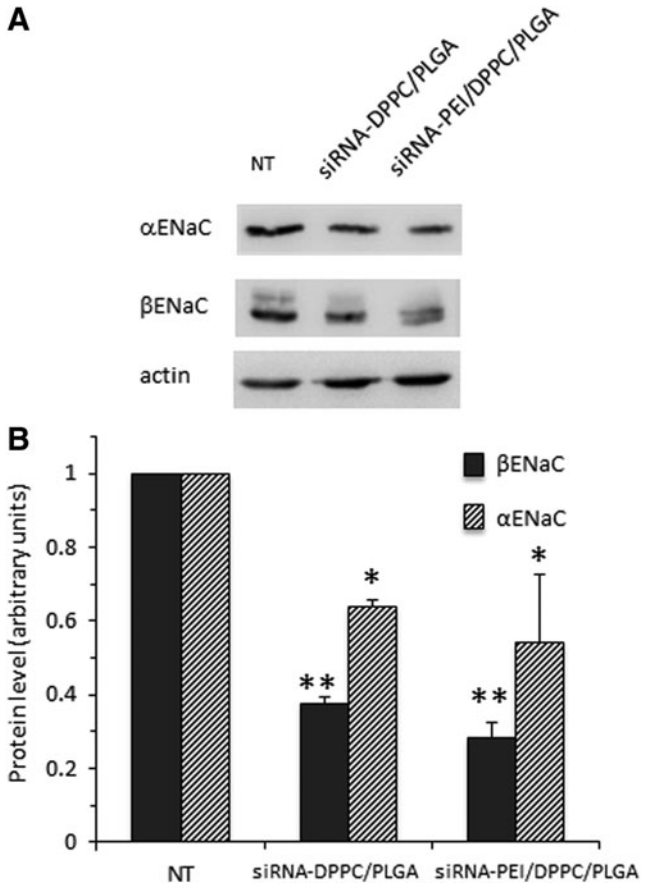

FIG. 8. Representative Western blotting of protein extracts from A549 cells treated or not with siRNA- DPPC/PLGA or siRNA-PEI/DPPC/PLGA for 72 hours. αENaC and βENaC proteins were detected by using the indicated antibodies. Anti-actin was used as the loading control **(A)**. The quantification of signals is shown **(B)**. The signal of untreated cells (NT) was set as 1.

Discussion

The importance of lung barriers in determining the therapeutic efficacy of inhaled drugs in severe lung diseases, such as CF, is nowadays acknowledged.[7] A current paradigm suggests that only NPs with appropriate size and surface properties may overcome the complex mucus airway barrier and assist drug interactions with human airway epithelial cells.[25,26] This aspect is particularly crucial for siRNA-based therapeutics, the clinical application of which is further hindered by the short half-life *in vivo* and the low capability to penetrate cell membranes. To overcome these issues, we have designed and developed novel DPPC/PLGA hNPs, containing or not PEI as third component, suitable for pulmonary delivery of siRNA.

In line with literature data,[10] a DPPC layer is likely present on the surface of PLGA particles giving rise to a core-shell structure, which is independent of the presence of PEI. As demonstrated by hNP/mucus interaction studies, this structure results in non-mucoadhesive or muco-inert hNPs, reasonably able to easily penetrate across the airway mucus layer.[8,17] Furthermore, the adopted formulation conditions allowed the production of hNPs with a hydrodynamic diameter of 150 nm, which are expected to easily diffuse through the gel-like structure of the mucus.[25,27] Finally, aqueous hNPs were transformed into a solid long-term stable lyophilized powder, which can be reconstituted in saline and, likely, employed to co-administer a mucus rehydrating agent, that is mannitol.[24]

If DPPC, which is the principal component of the lung lining fluids, is expected to tune hNP interactions with the lung environment, the addition of PEI can play a crucial role for siRNA entrapment inside DPPC/PLGA hNPs. This hypothesis was confirmed by encapsulation studies performed on two siRNA sequences, for α and β ENaC subunits, which have been shown to produce a long-term reduction of transepithelial Na^+ currents and fluid absorption.[28] In particular, the combination of the two siRNA can expand the lung fluid volume *in vitro*.[29] Of note, siRNA was entrapped inside selected hNPs with high efficiency, particularly when PEI was coencapsulated. This effect could be likely ascribed to the formation of a complex between PEI, employed at the theoretical N/P ratio of 10, and siRNA.

Information about the presence of PEI/siRNA complexes inside hNPs could not be derived from SAXS spectra, due to the very low amounts of both components. Nevertheless, SAXS analysis clearly demonstrated that the role of PEI in the formulation is not to affect the overall particle morphology, except for a very slight decrease of the average size. On the other hand, the phospholipid component is possibly coating the PLGA particles, as suggested by TEM analysis. Furthermore,

independent of the presence of PEI inside the formulation, hNPs were stable inside artificial CF mucus at least for 12 hours, confirming, along with *in vitro* aerosol performance studies, the potential of the system for direct aerosolization on the mucus-lined human airway epithelial barrier.

In fact, to attain maximum siRNA availability at lung epithelial cells, where its target is located, the hNPs should (i) uniformly deposit on the airway epithelium in their stable form; (ii) penetrate inside the lung epithelial barrier; and (iii) interact with the lung epithelium, without compromising cell availability. To draw key information on all these points and to establish a priori target formulation parameters for siRNA delivery to human airway epithelium, the behavior of the developed DPPC/PLGA hNPs after deposition on triple cell co-cultures, which realistically mimic human airway epithelium environment, was investigated.

When grown on porous supports at ALI, human bronchial epithelial cells reproduce *in vivo* morphology and key physiologic processes, sometimes including tight junctions and basal and mucus cells.[19,30] Furthermore, direct deposition of the aerosolized drug to the apical compartment of the cell culture can be envisaged through systems especially designed for dose-controlled and spatially uniform deposition of liquid aerosols on cells,[31,32] such as the Vitrocell Cloud employed in this study. Results showed that the adopted formulation conditions allowed to tune hNP properties, so as to achieve uniform and efficient aerosolization on lung epithelial cells in their integer form. Afterward, hNPs were demonstrated to penetrate inside extracellular lung lining fluids, to be taken up by lung epithelial cells without exerting a cytotoxic effect or a proinflammatory response on the treated lung epithelium model.

Once siRNA molecules overcome the aforementioned lung epithelial barriers and reach the target cells, they still need to overcome a series of intracellular barriers to exert their activity. Following cell entry, siRNA molecules must escape early from endosomes to avoid exposure to the noxious acidic environment as well as late-stage attack by the hydrolases in the endolysosome.[4] Noteworthy, *in vitro* ENaC silencing studies ruled out any degradation process, while proving the ability of the siRNA released from hNPs to reach the cytoplasm and, after binding to its target mRNA, to silence the gene of interest. As a consequence, robust and long-lasting knockdown of both αENaC and βENaC proteins could be achieved.

Conclusions

In this work, we have successfully designed and developed novel hNPs comprising PLGA likely surrounded by a DPPC shell, showing size and surface properties optimized for siRNA transport and delivery at lung. Optimized formulations allowed the encapsulation of a combination of siRNA against α and β subunits of ENaC channel with high efficiency, which could be optimized by the addition of PEI inside the formulation. The developed hNPs were muco-inert and stable inside AM. Stable hNP-based dry powders were produced by freeze-drying with mannitol, an osmotic agent of interest for CF treatment. Cell uptake studies upon *in vitro* aerosolization on TCCC confirmed the ability of fluorescently labeled hNPs to be internalized inside the airway epithelial barrier. Hazard assessment of hNPs demonstrated that the developed system does not exert cytotoxic or acute proinflammatory effect toward any of the cell components of the co-culture model. Finally, *in vitro* gene silencing studies highlighted that released siRNAs are capable to reduce ENaC protein expression in human lung epithelial cells. Overall, results demonstrate the great potential of DPPC/PLGA hNPs as carriers for siRNA delivery on the human epithelial airway barrier, prompting toward investigation of their therapeutic effectiveness in severe lung diseases.

Acknowledgments

F.U. gratefully acknowledges Compagnia di San Paolo and Istituto Banco di Napoli—Fondazione (STAR Program, Junior Principal Investigator Grant 2013, Napoli_call2013_35) for financial support. G.C. wishes to thank the International Society for Aerosols in Medicine (ISAM) for the 2015 ISAM Student Fellowships. E.D., A.P.F., and B.R.R. acknowledge the financial support of the Adolphe Merkle Foundation. The authors are grateful to Dr. T. Nrayanan, Dr. J. Moller, and to the ID02 beamline staff at the European Synchrotron Facility (Grenoble, France) and to Dr. Laetitia Haenni and Dr. Christoph Monnier at TEM facility of the Adolphe Merkle Institute for precious technical assistance.

Author Disclosure Statement

No competing financial interests exist.

References

1. Burnett JC, Rossi JJ, and Tiemann K: Current progress of siRNA/shRNA therapeutics in clinical trials. Biotechnol J. 2011;6:1130–1146.
2. Lee SH, Kang YY, Jang HE, and Mok H: Current preclinical small interfering RNA (siRNA)-based conjugate systems for RNA therapeutics. Adv Drug Deliv Rev. 2016; 104:78–92.
3. Karras JG, Sun G, Tay J, and Jackson AL: Reflections on microRNAs in chronic pulmonary disease: Looking into the miR-ror and crystal ball. Inflamm Allergy Drug Targets. 2013;12:88–98.
4. Lam JK, Liang W, and Chan HK: Pulmonary delivery of therapeutic siRNA. Adv Drug Deliv Rev. 2012;64:1–15.
5. Merkel OM, Rubinstein I, and Kissel T: siRNA delivery to the lung: What's new? Adv Drug Deliv Rev. 2014;75:112–128.
6. Ungaro F, d'Angelo I, Miro A, La Rotonda MI, and Quaglia F: Engineered PLGA nano- and micro-carriers for pulmonary delivery: Challenges and promises. J.Pharm Pharmacol. 2012;64:1217–1235.
7. d'Angelo I, Conte C, La Rotonda MI, Miro A, Quaglia F, and Ungaro F: Improving the efficacy of inhaled drugs in cystic fibrosis: Challenges and emerging drug delivery strategies. Adv Drug Deliv Rev. 2014;75:92–111.
8. d'Angelo I, Casciaro B, Miro A, Quaglia F, Mangoni ML, and Ungaro F: Overcoming barriers in *Pseudomonas aeruginosa* lung infections: Engineered nanoparticles for local delivery of a cationic antimicrobial peptide. Colloids Surf B Biointerfaces. 2015;135:717–725.
9. Griffiths PC, Cattoz B, Ibrahim MS, and Anuonye JC: Probing the interaction of nanoparticles with mucin for drug delivery applications using dynamic light scattering. Eur J Pharm Biopharm. 2015;97:218–222.
10. Raemdonck K, Braeckmans K, Demeester J, and De Smedt SC: Merging the best of both worlds: Hybrid lipid-enveloped

matrix nanocomposites in drug delivery. Chem Soc Rev. 2014;43:444–472.
11. Pandita D, Kumar S, and Lather V: Hybrid poly(lactic-co-glycolic acid) nanoparticles: Design and delivery prospectives. Drug Discov Today 2015;20:95–104.
12. Ungaro F, Giovino C, Coletta C, Sorrentino R, Miro A, and Quaglia F: Engineering gas-foamed large porous particles for efficient local delivery of macromolecules to the lung. Eur J Pharm Sci. 2010;41:60–70.
13. De Stefano D, Ungaro F, Giovino C, Polimeno A, Quaglia F, and Carnuccio R: Sustained inhibition of IL-6 and IL-8 expression by decoy ODN to NF-kappaB delivered through respirable large porous particles in LPS-stimulated cystic fibrosis bronchial cells. J Gene Med. 2011;13:200–208.
14. Blank F, Rothen-Rutishauser B, and Gehr P: Dendritic cells and macrophages form a transepithelial network against foreign particulate antigens. Am J Respir Cell Mol Biol. 2007; 36:669–677.
15. Maiolino S, Moret F, Conte C, Fraix A, Tirino P, Ungaro F, Sortino S, Reddi E, and Quaglia F: Hyaluronan-decorated polymer nanoparticles targeting the CD44 receptor for the combined photo/chemo-therapy of cancer. Nanoscale. 2015; 7:5643–5653.
16. Narayanan T, Diat O, and B+Âsecke P: SAXS and USAXS on the high brilliance beamline at the ESRF. Nuclear Instruments and Methods in Physics Research Section A: Accelerators, Spectrometers, Detectors and Associated Equipment 2001;467–468, Part 2:1005–1009.
17. Ungaro F, d'Angelo I, Coletta C, d'Emmanuele di Villa Bianca R, Sorrentino R, Perfetto B, Tufano MA, Miro A, La Rotonda MI, and Quaglia F: Dry powders based on PLGA nanoparticles for pulmonary delivery of antibiotics: Modulation of encapsulation efficiency, release rate and lung deposition pattern by hydrophilic polymers. J Control Release. 2012;157:149–159.
18. Marple VA, Olson BA, Santhanakrishnan K, Roberts DL, Mitchell JP, and Hudson-Curtis BL: Next generation pharmaceutical impactor: A new impactor for pharmaceutical inhaler testing. Part III. extension of archival calibration to 15 L/min. J Aerosol Med. 2004;17:335–343.
19. Lehmann AD, Daum N, Bur M, Lehr CM, Gehr P, and Rothen-Rutishauser BM: An in vitro triple cell coculture model with primary cells mimicking the human alveolar epithelial barrier. Eur J Pharm Biopharm. 2011;77:398–406.
20a. Russo A, Saide A, Cagliani R, Cantile M, Botti G, and Russo G: rpL3 promotes the apoptosis of p53 mutated lung cancer cells by down-regulating CBS and NFκB upon 5-FU treatment. Sci Rep. 2016;6:38369.
20b. Pagliara V, Saide A, Mitidieri E, d'Emmanuele di Villa Bianca R, Sorrentino R, Russo G, and Russo A: 5-FU targets rpL3 to induce mitochondrial apoptosis via cystathionine-β-synthase in colon cancer cells lacking p53. Oncotarget. 2016;7:50333–50348.
21. De Filippis D, Russo A, De SD, Cipriano M, Esposito D, Grassia G, Carnuccio R, Russo G, and Iuvone T: Palmitoylethanolamide inhibits rMCP-5 expression by regulating MITF activation in rat chronic granulomatous inflammation. Eur J Pharmacol. 2014;725:64–69.
22. Guinier G, and Fournet G: *Small Angle Scattering of X-Rays*. John Wiley & sons, New York, 1955. pp. 126–160.
23. Fonte P, Reis S, and Sarmento B: Facts and evidences on the lyophilization of polymeric nanoparticles for drug delivery. J Control Release 2016;225:75–86.
24. Nolan SJ, Thornton J, Murray CS, and Dwyer T: Inhaled mannitol for cystic fibrosis. Cochrane Database Syst Rev. 2015;10:CD008649.
25. Ensign LM, Tang BC, Wang YY, Tse TA, Hoen T, Cone R, and Hanes J: Mucus-penetrating nanoparticles for vaginal drug delivery protect against herpes simplex virus. Sci Transl Med. 2012;4:138–179.
26. d'Angelo I, Conte C, Miro A, Quaglia F, and Ungaro F: Pulmonary drug delivery: A role for polymeric nanoparticles? Curr Top Med Chem. 2015;15:386–400.
27. Lai SK, Wang YY, Hida K, Cone R, and Hanes J: Nanoparticles reveal that human cervicovaginal mucus is riddled with pores larger than viruses. Proc Natl Acad Sci U S A. 2010;107:598–603.
28. Caci E, Melani R, Pedemonte N, Yueksekdag G, Ravazzolo R, Rosenecker J, Galietta LJ, and Zegarra-Moran O: Epithelial sodium channel inhibition in primary human bronchial epithelia by transfected siRNA. Am J Respir Cell Mol Biol. 2009;40:211–216.
29. Gianotti A, Melani R, Caci E, Sondo E, Ravazzolo R, Galietta LJ, and Zegarra-Moran O: Epithelial sodium channel silencing as a strategy to correct the airway surface fluid deficit in cystic fibrosis. Am J Respir Cell Mol Biol. 2013;49:445–452.
30. Rothen-Rutishauser BM, Kiama SG, and Gehr P: A three-dimensional cellular model of the human respiratory tract to study the interaction with particles. Am J Respir Cell Mol Biol. 2005;32:281–289.
31. Endes C, Schmid O, Kinnear C, Mueller S, Camarero-Espinosa S, Vanhecke D, Foster EJ, Petri-Fink A, Rothen-Rutishauser B, Weder C, and Clift MJ: An in vitro testing strategy toward mimicking the inhalation of high aspect ratio nanoparticles. Part FibreToxicol. 2014;11:40.
32. Endes C, Mueller S, Kinnear C, Vanhecke D, Foster EJ, Petri-Fink A, Weder C, Clift MJ, and Rothen-Rutishauser B: Fate of cellulose nanocrystal aerosols deposited on the lung cell surface in vitro. Biomacromolecules. 2015;16:1267–1275.

Received on January 3, 2017
in final form, July 26, 2017

Reviewed by:
Olivia Merkel
Sally-Ann Cryan

Address correspondence to:
Barbara Rothen-Rutishauser, PhD
Adolphe Merkle Institute
University of Fribourg
Chemin des Verdiers 4
Fribourg 1700
Switzerland

E-mail: barbara.rothen@unifr.ch

Francesca Ungaro, PhD
Department of Pharmacy
University of Napoli Federico II
Via D. Montesano 49
Napoli 80131
Italy

E-mail: ungaro@unina.it